Hindawi Publishing Corporation
Journal of Applied Mathematics
Volume 2012, Article ID 525431, 10 pages
doi:10.1155/2012/525431

Research Article

Spectral Ratios for Crack Detection Using P and Rayleigh Waves

Enrique Olivera-Villaseñor,[1] Norberto Flores-Guzmán,[2] Ernesto Pineda-León,[3] Jaime Núñez-Farfán,[1] Manuel Carbajal-Romero,[4] and Alejandro Rodríguez-Castellanos[1]

[1] *Instituto Mexicano del Petróleo, Eje Central Lázaro Cárdenas 152, Gustavo A. Madero, 07730 México, DF, Mexico*
[2] *Centro de Investigación en Matemáticas, Jalisco s/n, Mineral de Valenciana, 36240 Guanajuato, GTO, Mexico*
[3] *Instituto Politécnico Nacional, Escuela Superior de Ingeniería y Arquitectura, UP Zacatenco, 07738 México, DF, Mexico*
[4] *Instituto Politécnico Nacional, Escuela Superior de Ingeniería Mecánica y Eléctrica, UP Azcapotzalco, 02250 México, DF, Mexico*

Correspondence should be addressed to
Enrique Olivera-Villaseñor, oliveravillasenor.e@hotmail.com

Received 2 April 2012; Accepted 7 June 2012

Academic Editor: Kai Diethelm

We obtain numerical results to help the detection and characterization of subsurface cracks in solids by the application of P and Rayleigh elastic waves. The response is obtained from boundary integral equations, which belongs to the field of elastodynamics. Once the implementation of the boundary conditions has been done, a system of Fredholm integral equations of the second kind and order zero is found. This system is solved using the method of Gaussian elimination. Resonance peaks in the frequency domain allow us to infer the presence of cracks using spectral ratios. Several models of cracked media were analyzed, where effects due to different crack orientations and locations were observed. The results obtained are in good agreement with those published in the references.

1. Introduction

It is well known that the presence of cracks in structural components leads to integrity problems. Cracks in materials used in mechanical and civil engineering cause reduction in strength which leads to instability, leakage, or collapse depending on the cracked component.

The development of studies for the identification and characterization of cracks has its origins in a variety of areas, citing for example, Griffith (1921) [1]. The technological progress focused on nondestructive testing (NDT) of materials has led to the development of devices such as pulse generators and receivers that can reach frequencies as high as 200 MHz. On the other hand, the advances in theoretical and numerical models [2, 3] has proved to be useful for a joint interpretation with developments in the NDT field [4, 5]. An important overview of theoretical results in relation to the interaction of elastic waves with cracks can be seen in Zhang and Gross [6]. The identification and characterization of subsurface cracks and surface-breaking cracks using Rayleigh waves are of much interest in the industry, see for example, references [7–12]. Using resonant spectroscopy techniques, Zadler and Scales [13] and Fan et al. [14] concluded that the presence of microcracks in materials affects a wide range of mechanical properties including shear, bulk, and Young's modulus, for various levels of internal fracturing. Moreover, results of [13] suggest that bulk modulus is more sensitive to changes in crack density, while [14] points out that the Young's modulus is a function of crack damage parameter.

This paper considers the study of boundary integral equations, derived from the Somigliana classical theorem [15], to deal with the detection and characterization of subsurface discontinuities using P and Rayleigh waves. This method can be seen as one belonging to the boundary element method (BEM). It acquires the character of indirect (IBEM), because the unknown force densities in the integrant are obtained in an intermediate step. Subsequent to the implementation of the boundary conditions, a system of Fredholm integral equations of the second kind and order zero in the frequency domain is solved using the method of Gaussian elimination. It is important to mention that an analysis in frequency domain reveals resonance peaks, which can be linked to the presence of subsurface cracks.

2. Boundary Integral Equation

If an elastic solid domain V bounded by its boundary S is considered, the diffracted displacement and traction fields under harmonic excitation can be expressed, neglecting body forces, by means of the single-layer boundary integral equations

$$u_i^d(\mathbf{x}) = \int_{\partial S} G_{ij}(\mathbf{x},\xi)\phi_j(\xi)dS_\xi, \tag{2.1}$$

$$t_i^d(\mathbf{x}) = c\phi_i(\mathbf{x}) + \int_{\partial S} T_{ij}(\mathbf{x},\xi)\phi_j(\xi)dS_\xi, \tag{2.2}$$

where $u_i^d(\mathbf{x})$ = ith component of the displacement at point $\mathbf{x}$, $G_{ij}(\mathbf{x};\xi)$ = Green function, which represent the displacement produced in direction i at $\mathbf{x}$ due to the application of a unitary force in direction j at point ξ, $\phi_j(\xi)$ is the force density in the direction j at point ξ. The product $\phi_j(\xi)dS_\xi$ is the force distribution at the surface S (the subscripts i, j are limited to be 1 or 3). The subscript in the differential shows the variable over which the integration is done. This integral equation can be obtained from Somigliana representation [15]. Furthermore, it was demonstrated that if $\phi_j(\xi)$ is continuous along S, the displacement field is continuous across S [16]. $t_i^d(\mathbf{x})$ = ith component of tractions, $c = 0.5$ if $\mathbf{x}$ tends to the boundary S "from inside" the region, $c = -0.5$ if $\mathbf{x}$ tends S "from outside" the region, or $c = 0$ if $\mathbf{x}$ is not at S. $T_{ij}(\mathbf{x};\xi)$ = Green function traction, that is, the traction in i direction at point $\mathbf{x}$, due to the application

of a unitary force in j direction at ξ on S. The following section presents Green functions for displacements and tractions.

3. Two-Dimensional Green Functions in Unbounded Space

In a homogeneous isotropic elastic unbounded medium, 2D Green functions are the displacements and tractions responses of the medium at a given location $\mathbf{x}$ when a unit line load is applied at ξ.

Assuming harmonic time dependence, $\exp(i\omega t)$, where $i = \sqrt{-1}$, ω = circular frequency, and t = time, the displacement in i direction when the load is applied in jth direction can be expressed as

$$G_{ij}(\mathbf{x};\xi) = A\delta_{ij} - B\left(2\gamma_i\gamma_j - \delta_{ij}\right). \tag{3.1}$$

On the other hand, the tractions at $\mathbf{x}$ in i direction for a given unit vector n_i normal to S when the unit load is applied at ξ in the direction j are

$$\begin{aligned} T_{ij} = {} & \frac{\mu}{r}\left\{\left[-4B + \lambda\frac{D(\omega r/\alpha)}{2\mu\alpha^2}\right]\gamma_j n_i + \left[-4B + \frac{D(\omega r/\beta)}{2\beta^2}\right]\times\left[\gamma_i n_j + \gamma_k n_k \delta_{ij}\right]\right\} \\ & + \frac{\mu}{r}\left\{(C + 16B)\gamma_i\gamma_j\gamma_k n_k\right\}. \end{aligned} \tag{3.2}$$

For (3.1) and (3.2), these expressions are defined as follows:

$$\begin{aligned} A &= \frac{1}{i8\rho}\left[\frac{H_0^{(2)}(\omega r/\alpha)}{\alpha^2} + \frac{H_0^{(2)}(\omega r/\beta)}{\beta^2}\right], \\ B &= \frac{1}{i8\rho}\left[\frac{H_2^{(2)}(\omega r/\alpha)}{\alpha^2} - \frac{H_2^{(2)}(\omega r/\beta)}{\beta^2}\right], \\ C &= \frac{D(\omega r/\alpha)}{\alpha^2} - \frac{D(\omega r/\beta)}{\beta^2}, \\ D(p) &= \frac{i}{2\rho}pH_1^{(2)}(p), \end{aligned} \tag{3.3}$$

where λ and μ are Lamé's constants, ρ = mass density, and $\alpha = \sqrt{(\lambda + 2\mu)/\rho}$ and $\beta = \sqrt{\mu/\rho}$ are the P and S wave velocities, respectively, $r = \sqrt{(x_1 - \xi_1)^2 + (x_3 - \xi_3)^2}$, $\gamma_j = (x_j - \xi_j)/r$, δ_{ij} = Kronecker's delta (=1 if $i = j$, = 0 if $i \neq j$), and $H_m^{(2)}(\cdot)$ is the Hankel's function of second kind and order m.

4. Statement of the Problem

In general terms, the response of a cracked medium should satisfy the displacement and traction states represented by the sum of a free field (superscript "o") and a diffracted field

(superscript "d"), that is, $u_i(\mathbf{x}) = u_i^o(\mathbf{x}) + u_i^d(\mathbf{x})$ and $t_i(\mathbf{x}) = t_i^o(\mathbf{x}) + t_i^d(\mathbf{x})$, respectively. The free field always represents the incidence of P or Rayleigh waves. To represent the crack or discontinuity, tractions free boundary conditions must be established at its contour, that is, $t_i(\mathbf{x}) = 0$.

The integral equations established in (2.1) allow the inclusion of cracks or discontinuities, because of the use of multiregion concept, in which the domain of study may be discrete in regions, and the join between them is given by the boundary conditions that represent continuity ($u_i^R(\mathbf{x}) = u_i^E(\mathbf{x})$ and $t_i^R(\mathbf{x}) = t_i^E(\mathbf{x})$) for example, the union of the region R and the region E). To include a crack between two regions, traction-free boundary conditions $t_i^R(\mathbf{x}) = 0$ and $t_i^E(\mathbf{x}) = 0$ must be established for the discontinuity sides that belong to each region.

Each surface is divided in boundary elements of length equal to or less than $1/6$ of the shortest SV wavelength each, depending on the frequency. For example, for a free surface, the join between regions R and E and the discontinuity requires N, M, and K boundary elements, respectively, then, (2.1) must be written, considering free and diffracted fields and boundary conditions described previously, as follows:

$$
\begin{aligned}
c\phi_i^R(\mathbf{x}) + \int_{\partial R} \phi_j^R(\xi) T_{ij}^R(\mathbf{x};\xi)\, dS_\xi &= -t_i^{oR}(\mathbf{x}), \quad \mathbf{x} \in \partial_3 R,\\
\int_{\partial R} \phi_j^R(\xi) G_{ij}^R(\mathbf{x};\xi)\, dS_\xi - \int_{\partial E} \phi_j^E(\xi) G_{ij}^E(\mathbf{x};\xi)\, dS_\xi &= u_i^{oE}(\mathbf{x}) - u_i^{oR}(\mathbf{x}), \quad \mathbf{x} \in \partial_1 R = \partial_1 E,\\
c\phi_i^R(\mathbf{x}) + \int_{\partial R} \phi_j^R(\xi) T_{ij}^R(\mathbf{x};\xi)\, dS_\xi - c\phi_i^E(\mathbf{x}) - \int_{\partial E} \phi_j^E(\xi) T_{ij}^E(\mathbf{x};\xi)\, dS_\xi &= t_i^{oE}(\mathbf{x}) - t_i^{oR}(\mathbf{x}),\\
&\qquad \mathbf{x} \in \partial_1 R = \partial_1 E,\\
c\phi_i^R(\mathbf{x}) + \int_{\partial R} \phi_j^R(\xi) T_{ij}^R(\mathbf{x};\xi)\, dS_\xi &= -t_i^{oR}(\mathbf{x}), \quad \mathbf{x} \in \partial_2 R,\\
c\phi_i^E(\mathbf{x}) + \int_{\partial E} \phi_j^E(\xi) T_{ij}^E(\mathbf{x};\xi)\, dS_\xi &= -t_i^{oE}(\mathbf{x}), \quad \mathbf{x} \in \partial_2 E.
\end{aligned}
\tag{4.1}
$$

Region R is formed by the boundary $\partial R = \partial_1 R \cup \partial_2 R \cup \partial_3 R$, while the region E by the boundary $\partial E = \partial_1 E \cup \partial_2 E$. $\partial_1 R$ and $\partial_1 E$ represent the continuous segments between regions R and E, $\partial_2 R$ is the discontinuity or crack face in the side of the region R, $\partial_2 E$ is the discontinuity or crack face in the side of the region E, and $\partial_3 R$ is the free surface belonging to region R.

Equation (4.1) form a Fredholm system of integral equations to be solved. Once the unknown values (ϕ's) are obtained, the diffracted displacement and traction fields are computed by means of (2.1) and (2.2), respectively.

5. Validation and Numerical Examples

A reference has been selected to validate the results obtained by this integral formulation for a noncracked medium. Graff [17] shows analytic normalized displacements due to the incidence of Rayleigh waves versus normalized depth for two Poisson ratios ($\nu = 0.25$ and $\nu = 0.33$, see Figure 1). He mentions that the energy is located near the free surface and disappears at almost one Rayleigh wavelength (λ_R). Then, the effective use of Rayleigh waves for crack detection could be limited to shallow cracks. Graff [17] plots horizontal (h) and

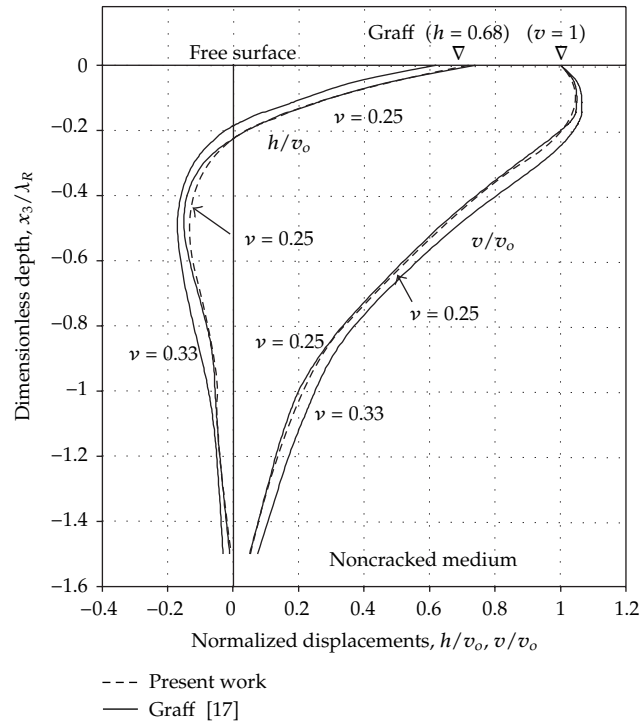

Figure 1: Normalized displacements versus normalized depth, where v_o is the value for the vertical displacement at the surface.

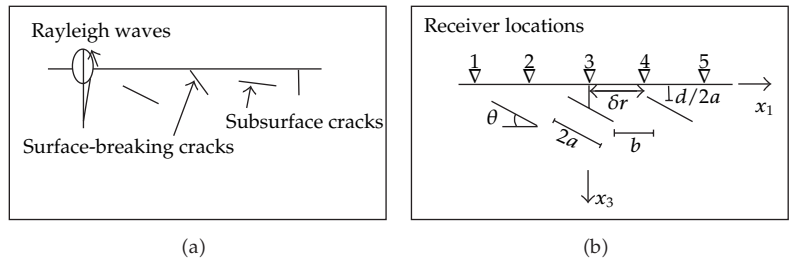

Figure 2: (a) Cracked medium under the incidence of Rayleigh waves, (b) Crack dimensions and receiver locations.

vertical (v) displacements and obtains the values of $h = 0.68$ and $v = 1.00$ at the free surface, for the Poisson ratio $\nu = 0.25$. Therefore, the spectral ratio for this case is $h/v = 0.68$. Figure 1 includes curves obtained in the present work for $\nu = 0.25$ (plotted with dashed line). Good agreement between the IBEM and Graff [17] is observed. Models of cracked media under the incidence of Rayleigh waves are illustrated in Figures 2(a) and 2(b).

To study the effect of cracks under the incidence of Rayleigh waves four depth ratios $d/2a = 0.2$, 0.4, 0.6 and 1.0, where d is crack depth and $2a$ is crack length, were selected. The frequency analysis was carried out for the range $0 \leq \eta \leq 3.0$, where $\eta = \omega d/C_R$, ω is the circular frequency, and C_R represents the Rayleigh wave velocity. A Poisson solid ($\nu = 0.25$) was considered. Horizontal and vertical displacements measured at point A (see detail in

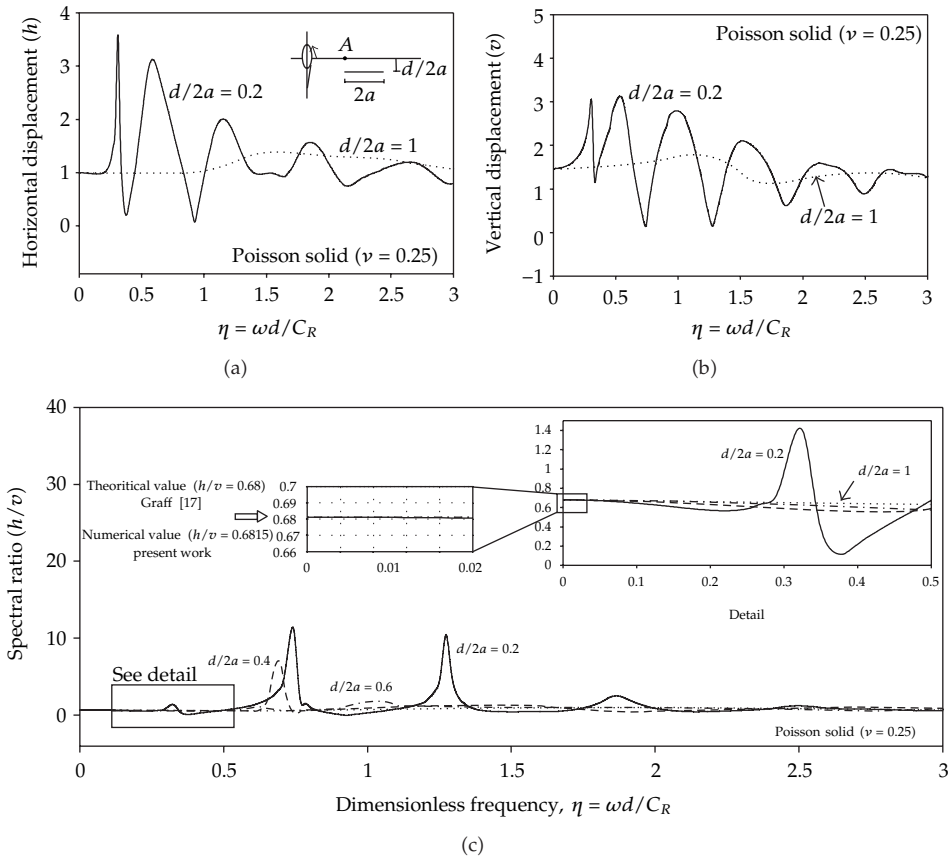

Figure 3: Cracks subjected to the incidence of Rayleigh waves. (a) Horizontal displacements for crack depth ratios $d/2a = 0.2$ and $d/2a = 1.0$, (b) Vertical displacements for crack depth ratios $d/2a = 0.2$ and $d/2a = 1.0$, (c) Spectral ratio h/v for crack depths $d/2a = 0.2$, 0.4, 0.6 and 1.0.

Figure 3(a)) are shown in Figures 3(a) and 3(b), respectively, for the shallowest ($d/2a = 0.2$) and the deepest ($d/2a = 1.0$) crack. It is expected that a shallow crack causes major alterations to Rayleigh wave front, while a deep crack has an effect almost negligible for both displacements.

Figure 3(c) shows a spectral ratio h/v almost constant for all depth ratios, except for crack depths $d/2a = 0.2$ and $d/2a = 0.4$. In the amplified detail of Figure 3(c), it can be observed that the first peak is caused by crack depth $d/2a = 0.2$, as well as the constant behavior shown for crack depth $d/2a = 1.0$, additionally, it can be seen that at low frequencies the spectral ratio h/v tends to 0.6815 for any crack depth, moreover, this value is maintained even for the case when there is no crack, see also Figure 1 for values $h = 0.68$ and $v = 1.00$ on the surface (then $h/v = 0.68$) obtained by Graff [17]. The agreement is excellent.

Spectral ratios to observe the influence of crack orientation are plotted in Figure 4. Here, the crack has an angle $\theta = 45°$ (descending crack) and $\theta = 135°$ (ascending crack) and a depth ratio $d/2a = 0.1$, for both cases. Spectral ratios for five receivers are displayed, the distance increment between them is $\delta r = 2$. Important aspects emerge from these cases studied. Descending crack (continuous line) causes energy splitting to the interior of the medium. For this reason, the receivers 4 and 5 do not show wave interactions between

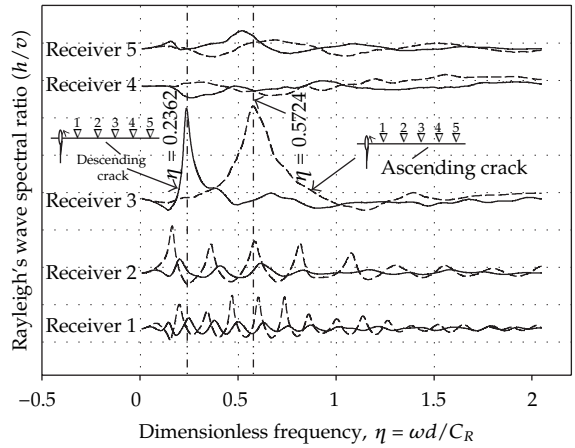

Figure 4: Rayleigh wave spectral ratios for ascending (dashed line) and descending (continuous line) cracks, for a Poisson solid.

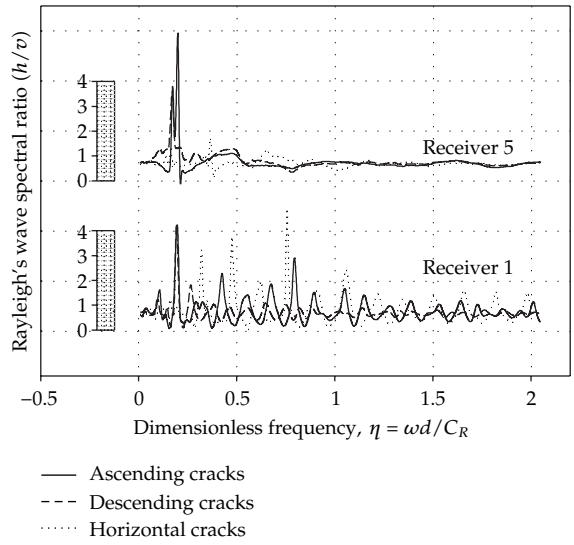

Figure 5: Rayleigh wave spectral ratio for ascending, descending, and horizontal cracks in multicracked media.

the crack and the free surface. These interactions are clearly observed for receivers 1 and 2. Similar behavior can be seen for ascending crack (dashed line), except that wave reflections are very evident for receivers 1 and 2. For receiver 3, significant resonance peaks are present. For the case of descending cracks a strong amplification is obtained at $\eta = 0.2362$, while for ascending cracks this peak is observed at $\eta = 0.5724$. This fact implies that resonance peaks presented in the h/v ratios may depend on the direction in which Rayleigh wave travels, therefore, the same crack, practically, can show different patterns. Following this remark, an analysis of crack orientation for several angles was carried out, and results are presented in Figure 6.

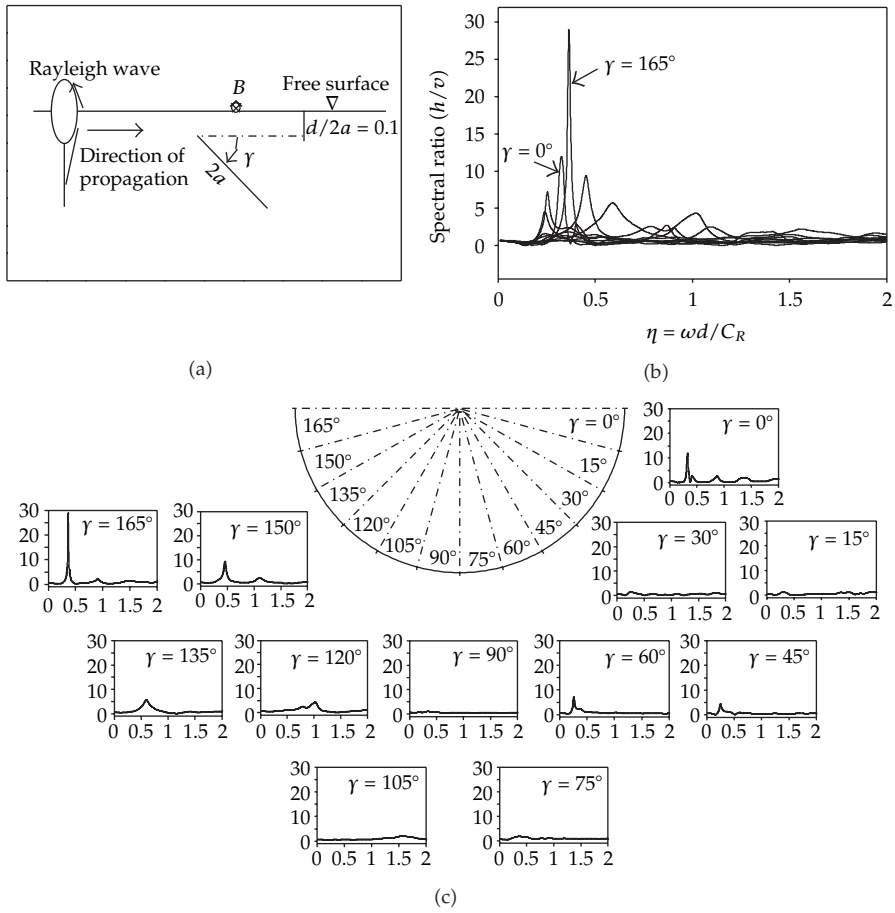

Figure 6: Effect of crack orientation. (a) model studied, (b) spectral ratio, (c) detailed response for several crack orientations.

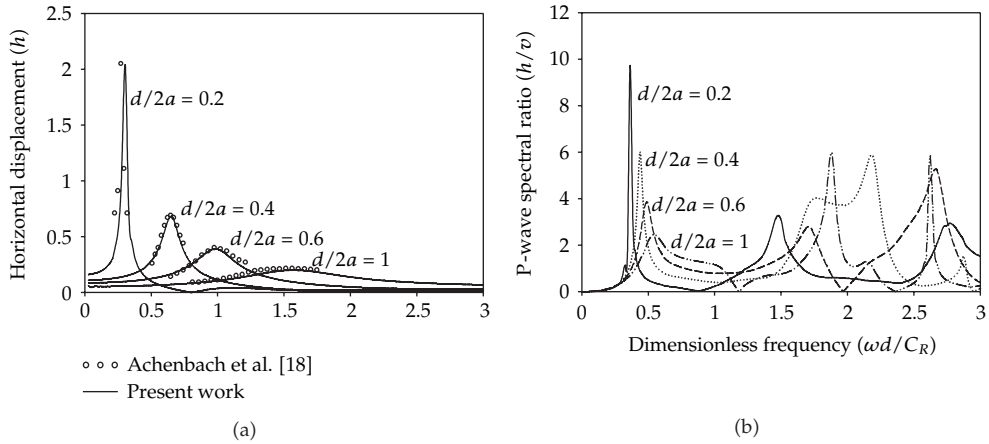

Figure 7: Cracked medium under P-wave incidence. (a) Validation of the problem, (b) P-wave spectral ratio for four crack depth ratios.

To observe the h/v spectral ratios due to multiple cracking, systems of three cracks were modeled. Now, three consecutive ascending ($\theta = 135°$), descending ($\theta = 45°$), or horizontal ($\theta = 0°$) cracks were considered, and the spectral ratios measured for the receivers 1 and 5 only. The distance from receiver 1 to 5 is $32/2a$, $d/2a = 0.1$, $b/2a = 0.7171$ (see Figure 2(b)) for nonhorizontal cracks and $b/2a = 1.0$ for horizontal cracks. In Figure 5, descending cracks (dashed line) display a few wave interactions for both receivers, as expected. However, ascending (continuous line) and horizontal (dotted line) cracks show more waves interacting between the up-crack face and the free surface. This effect is more evident in receiver 1. In all cases, receiver 5 shows an attenuated response for high frequencies.

As mentioned above, resonance peaks caused by the incidence of Rayleigh waves are stronger for some given directions of propagation or crack orientations. This characteristic may cause problems when identifying or characterizing cracks is required. Therefore, a crack could present evident resonance peaks when subjected to a given direction of Rayleigh waves, while, the same crack may not present important resonance peaks for other incidence or crack orientation. Figure 6 plots spectral ratios calculated at point B for twelve crack orientations according to Figure 6(a). Spectral ratios are graphed in Figure 6(b), while the detailed response for each angle of incidence is illustrated in Figure 6(c). It is remarkable that horizontal or almost horizontal cracks make sharp peaks appear. The maximum h/v ratio is obtained for $\gamma = 165°$ reaching a spectral ratio $h/v = 30$. The vertical crack shows an almost constant value.

Finally, spectral ratios for the case of P-wave incidence are presented. In Figure 7(a) the validation of this integral formulation is shown, horizontal displacements calculated at point A (see Figure 3(a)) are compared. The same crack depths and frequency range were considered. As mentioned above, shallow cracks displays sharp peaks, and these tend to be negligible as the crack depth increases. Our results show good agreement with those obtained by Achenbach et al. [18]. Spectral ratios for these analyses are depicted in Figure 7(b), where several resonance peaks appear. Lower resonant effects are observed for the deeper crack. Moreover, spectral ratios could be considered as a way to identify and characterize subsuperficial cracks

6. Conclusions

The present work deals with the detection and characterization of subsurface cracks in solids by the application of P and Rayleigh elastic waves. The response is obtained from boundary integral equations, which belongs to the field of elastodynamics. After the implementation of the boundary conditions and the use of the multiregion concept, it was possible to formulate a system of integral equations, where the unknowns named as force densities were obtained. This method is understood as an indirect boundary element formulation or IBEM and can be seen as a conceptualization of Somigliana classical theorem. The excitation of the system was carried out by the incidence of Rayleigh waves leading to spectra that is useful for the characterization of embedded cracks in solids.

The results obtained in the present work were validated with published results of Graff [17] for noncracked medium and with Achenbach et al. [18] for a cracked one. The presence of cracks or discontinuities causes resonance peaks, which can be identified using frequency analysis; the resonance peaks are sharper as the defects are shallower. Moreover, it was noticed that a crack could present evident resonance peaks when this is subjected to a given

direction of excitation, while the same crack may not present important resonance peaks for other incidence or crack orientation. This integral formulation can deal with complex crack shapes or free-surface geometries, which is an advantage of this method.

References

[1] A. A. Griffith, "The phenomena of rupture and flow in solids," *Philosophical Transactions of the Royal Society A*, vol. 221, pp. 163–197, 1921.

[2] L. B. Freund, "Crack propagation in an elastic solid subjected to general loading-III. Stress wave loading," *Journal of the Mechanics and Physics of Solids*, vol. 21, no. 2, pp. 47–61, 1973.

[3] J. D. Achenbach, Y. C. Angel, and W. Lin, *Wave Propagation in Homogeneous Media and Ultrasonic Nondestructive Evaluation*, Edited by G. C. Johnson, ASME, New York, NY, USA, 1984.

[4] D. E. Bray and R. K. Stanley, *Nondestructive Evaluation, a Tool in Design, Manufacturing and Service*, CRC Press, Boca Raton, Fla, USA, 1997.

[5] J. A. Scales and K. Van Wijk, "Multiple scattering attenuation and anisotropy of ultrasonic surface waves," *Applied Physics Letters*, vol. 74, no. 25, pp. 3899–3901, 1999.

[6] C. H. Zhang and D. Gross, *On Wave Propagation in Elastic Solids with Cracks*, vol. 2 of *International Series on Advances in Fracture Mechanics*, Computational Mechanics Publications, Southampton, UK, 1998.

[7] W. R. Tweddell, "Frequency spectral analysis of Rayleigh waves to size surface-breaking cracks," *Materials Evaluation*, vol. 48, no. 11, pp. 1348–1349, 1990.

[8] C. M. Van Der Kolk, W. S. Guest, and J. H. H. M. Potters, "The 3D shear experiment over the Natih field in Oman: the effect of fracture-filling fluids on shear propagation," *Geophysical Prospecting*, vol. 49, no. 2, pp. 179–197, 2001.

[9] M. Ochiai, D. Lévesque, R. Talbot, A. Blouin, A. Fukumoto, and J. P. Monchalin, "Detection and characterization of discontinuities in stainless steel by the laser ultrasonic synthetic aperture focusing technique," *Materials Evaluation*, vol. 62, no. 4, pp. 450–459, 2004.

[10] B. Masserey and E. Mazza, "Analysis of the near-field ultrasonic scattering at a surface crack," *Journal of the Acoustical Society of America*, vol. 118, no. 6, pp. 3585–3594, 2005.

[11] B. Masserey, L. Aebi, and E. Mazza, "Ultrasonic surface crack characterization on complex geometries using surface waves," *Ultrasonics*, vol. 44, supplement, pp. e957–e961, 2006.

[12] J. K. Na and J. L. Blackshire, "Interaction of Rayleigh surface waves with a tightly closed fatigue crack," *NDT and E International*, vol. 43, no. 5, pp. 432–439, 2010.

[13] B. J. Zadler and J. A. Scales, "Monitoring crack-induced changes in elasticity with resonant spectroscopy," *Journal of Applied Physics*, vol. 104, no. 2, Article ID 023536, 4 pages, 2008.

[14] X. Fan, E. D. Case, and M. J. Baumann, "The effect of indentation-induced microcracks on the elastic modulus of hydroxyapatite," *Journal of Materials Science*, vol. 47, no. 17, pp. 6333–6345, 2012.

[15] F. J. Sanchez-Sesma and M. Campillo, "Diffraction of *P, SV* and Rayleigh waves by topographic features: a boundary integral formulation," *Bulletin—Seismological Society of America*, vol. 81, no. 6, pp. 2234–2253, 1991.

[16] V. D. Kupradze, "Dynamical problems in elasticity," in *Progress in Solid Mechanics*, I. N. Sneddon and R. Hill, Eds., North-Holland, Amsterdam, The Netherlands, 1963.

[17] K. F. Graff, *Wave Motion in Elastic Solids*, Ohio State University Press, 1975.

[18] J. D. Achenbach, W. Lin, and L. M. Keer, "Surface-waves due to scattering by a near-surface parallel crack," *IEEE Transactions on Sonics and Ultrasonics*, vol. 30, no. 4, pp. 270–276, 1983.